

SIMULATIONS OF DIAMOND DETECTORS WITH SCHOTTKY CONTACTS*

G. I. Bell[†], D. Dimitrov, S. Zhou, D. Meisner, J. Cary, D. Smithe, Tech-X Corp, Boulder, CO, 80303, USA
J. Smedley, Brookhaven National Lab, Upton, NY, 11973, USA
E. Muller, M. Gaowei, Stony Brook University, Stony Brook, NY, 11794, USA

Abstract

We present simulations of semiconductor devices using the code VSim (formerly Vorpal). The 3D simulations involve the movement and scattering of electrons and holes in the semiconductor, voltages which may be applied to external contacts, and self-consistent electrostatic fields inside the device. Particles may experience a Schottky barrier when moving between the semiconductor and a metal contact. Example devices include MOSFETs as well as a diamond X-ray detector. Our code VSim includes scattering models for GaAs and diamond, and runs in parallel on thousands of processors. We compare our simulation results with experimental results from a prototype diamond X-ray detector.

INTRODUCTION

Diamond is a promising material for use in X-ray and particle detectors [1]. Figure 1 shows the experimental

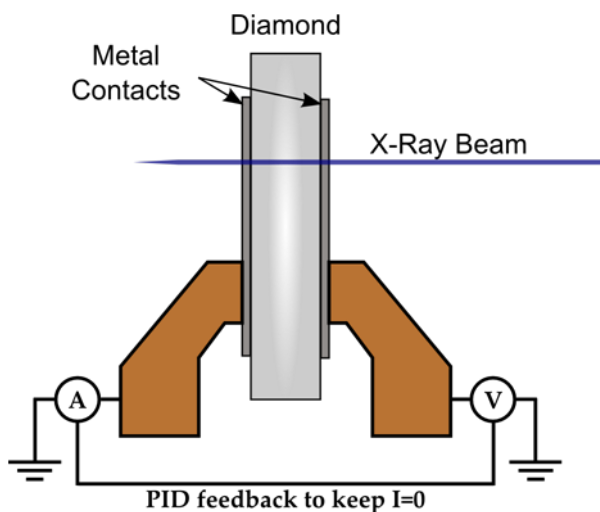


Figure 1: Schematic of an experimental X-ray detector.

setup, using a thin sheet of diamond 90 μm thick. When an X-ray photon passes through this thin diamond sheet, it may be absorbed, creating an electron-hole pair. The electron and hole scatter inelastically in diamond, creating many more secondary electrons and holes. Further relax-

ation of low energy charge carriers is dominated by scattering with phonons.

If a voltage bias is applied between the metal contacts, the generated electrons and holes drift in opposite directions and become separated. Diffusion also affects both charge carriers, and with the voltages applied experimentally (up to 8 V across the metal contacts) the effects of drift and diffusion are similar in magnitude. A charge carrier will drift at a constant rate due to the applied field, while the average distance traveled as a result of diffusion scales as the square root of the elapsed time. When these charge carriers reach the metal contacts, they may be absorbed, generating a net current. In order to reach the metal contacts, electrons and holes must cross a potential barrier.

Modeling this detector requires that we resolve widely disparate time scales. In order to accurately model the high-energy electrons produced in the initial X-ray absorption, we must resolve the mean time between inelastic collisions, on the order of 10^{-17} seconds. On the other hand the low energy electrons and holes interact with phonons much less frequently, about once every 10^{-14} seconds. Finally, the time needed for an electron or hole to drift or diffuse across 90 μm is around 10^{-8} seconds (10 ns). There are nine orders of magnitude between the smallest time scale of the simulation and the final time, so we can't simulate all these processes for 10 ns.

In contrast to the experiments, in these simulations we consider the delta-function response of the detector to a single photon—or, for better statistics, many photons all absorbed by the device at time $t = 0$.

SIMULATION OF A DIAMOND DETECTOR WITHOUT BARRIERS

In order to understand the role played by a Schottky barrier (which can prevent charge carriers from exiting through the metal contacts) we first simulate a diamond detector without barriers.

Our 3D simulations of the diamond detector use a domain of size $90 \times 20 \times 20 \mu\text{m}$, and we use periodic boundaries in y and z . The electrostatic field is calculated at each time step by doing a Poisson solve based on the current charge density, with boundary conditions in x using the applied voltage difference.

We consider 500 photons, each with an energy of 3 KeV, and absorbed by the diamond detector at $t = 0$. In diamond 3 KeV X-rays have an absorption length of 31.6 μm [2]. In order to determine the initial x position of the primary elec-

*This work is supported by the US DOE Office of Science, department of Basic Energy Sciences, grant numbers DE-SC0006246 and DE-SC0007577.

[†] gibell@txcorp.com

tron and hole, we sample from an exponential distribution with a decay length of 31.6 μm . The initial transverse position is chosen uniformly across the domain width. The hole energy was obtained by sampling from a uniform distribution between 0 and 23 eV, the width of the diamond valence band. The electron energy was then determined by conservation of energy.

The beam enters from the right (of Figure 1) and due to the absorption length more than 80% of the primary electrons and holes are located in the right half of the domain. During the first phase of the simulation, inelastic scattering generates secondary electrons in the conduction band and holes in the valence band. To simulate this phase we use our implementation [3] of the Tanuma–Powell–Penn [4] optical model for inelastic scattering in diamond at 300K. The time step during this phase is a fraction of the inelastic mean free path, $\Delta t = 8.33 \times 10^{-18}$ sec.

After 0.25 picoseconds (30,000 time steps), the generation of secondary electrons and holes is complete. We then enter the second phase of the simulation, dominated by low-energy inelastic scattering with phonons. We have implemented [3] the models of Jacoboni and Reggiani [5]. In this phase the time step is $\Delta t = 5 \times 10^{-15}$ sec.

To calculate the current in our simulations, when an electron or hole is absorbed by a contact, we record the time in a history log. Let $h_\ell(t)$ be the number of holes which have been absorbed by the left contact during the time interval $(0, t)$, and similarly with $e_\ell(t)$ for electrons. Then the total accumulated charge in the left contact at time t is

$$Q_\ell = (h_\ell - e_\ell)q \quad (1)$$

where $q \approx 1.6 \times 10^{-19}$ coulomb is the elementary charge. The analogous quantity for the right contact is Q_r . The current at time t is then the time derivative of $Q_\ell - Q_r$, and the average current during the time interval $(0, t)$ is $(Q_\ell(t) - Q_r(t))/t$. In our simulations, the average current is linear in the applied voltage (Figure 2).

We can estimate the average current using the number of charge carriers generated by the absorption of 500 photons combined with their drift rate. We start with an average energy required to generate an electron-hole pair of 13.8 eV. This figure comes from X-ray measurements [6, 7] and has been verified for our model in previous simulations [3]. Using this average energy, we predict that 500 photons at 3 KeV will generate around 1.1×10^5 hole-electron pairs.

The drift speed of electrons and holes is approximately linear in the applied electric field [3]. In reality, electrons and holes drift at slightly different rates, but we will ignore any difference in this estimate. For the voltages in these simulations, the applied field is less than 0.1 MV/m. In these weak electric fields, the drift speed d is well approximated by [3],

$$d \approx \left(0.2 \frac{m^2}{V \cdot \text{sec}}\right) F \quad (2)$$

where F is the electric field strength in V/m. For example, a bias voltage of 4 V over 90 μm gives $F = 44.4$ KV/m

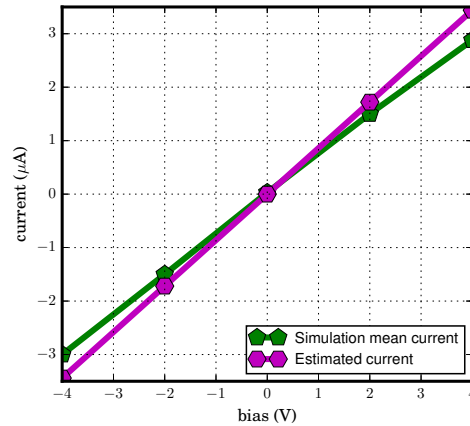


Figure 2: Average current with no barrier. The estimated current comes from a drift rate which is linear in the applied field, equation (2).

and a drift speed $d = 8900$ m/sec. At this rate it takes an electron or hole 10 ns to drift across the entire domain.

Combining the number of e-h pairs generated with the time needed to cross 90 μm , we estimate that a voltage bias of 4 V will generate an average current of 3.3 μA . Because the drift rate is linear in the applied field, so is the estimated current, (Figure 2, purple line).

The curves in Figure 2 show the immediate response of the detector to the absorption of 500 photons. In a steady state situation, we do not expect a linear relationship between current and voltage bias, because the current is limited by the rate at which photons are absorbed. As the voltage bias is increased we expect that the current will saturate at some limiting value. For example, suppose 3 KeV photons are absorbed by the detector at a constant rate of 4×10^{10} per second. Using an average of 13.8 eV to generate each electron-hole pair, and assuming all charge carriers hit the boundaries and generate current, we obtain a maximum steady state current (for any voltage) of 2.8 μA .

SIMULATION OF SCHOTTKY CONTACTS

In reality, for a charge carrier to enter a metal contact at the edge of the simulation, it must cross a potential barrier. The barrier is more significant for electrons compared to holes, at the moment we include the potential barrier only for electrons. In order to calculate the probability that an electron will pass through the barrier, we use the transfer matrix method [8, 9, 10], which has been implemented in VSim [11].

As an electron approaches a metal contact at $x = 0$ from the left, it sees a potential barrier $V(x)$ given by

$$V(x) = \begin{cases} 0 & x < 0 \\ V_0 + (V_1 - V_0)H(x - d) - Fx & x \geq 0 \end{cases} \quad (3)$$

where V_0 is the height of the barrier, taken as 0.35 eV, and d is the width of the barrier, taken as 8 Å. Here V_1 is the height of the potential after the barrier, taken as 0.18 eV, and F is the strength of the applied electric field expressed as eV/m. This model was created to simulate emission of electrons from diamond into vacuum [11]. In our simulations when an electron passes the barrier into the metal contact it is removed. At the moment we do not model the possibility than an electron or hole may pass from the metal contact back into diamond.

In these simulations, some electrons are able to pass the barrier during the first phase, but in the second phase almost all electrons have insufficient energy to pass the barrier. Instead, the electrons accumulate in the diamond near the right contact (under positive bias), or near the left contact (under negative bias), where they reduce the electric field and thereby charge carrier drift rates. All simulations were run for at least 1 ns, around 250,000 time steps.

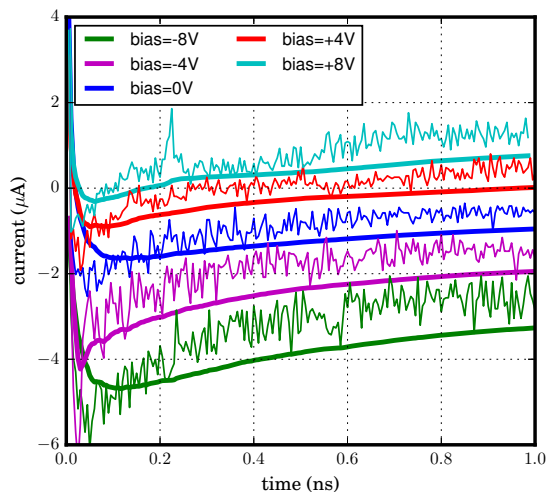


Figure 3: Current vs. time for bias -8 V to +8 V. The thin lines show the instantaneous current at time t , while the thick lines show the average current during $(0, t)$.

Holes are primarily responsible for the current shown in Figure 3. After the first phase is completed, the current is always negative for the first 0.1 ns, even when the voltage bias is positive (up to 8 V). During this time electrons near the right edge of the simulation have too little energy to cross the barrier, while some holes diffuse into the right contact, even when the electric field is against them. The gradual rise in current seen in Figure 3 after 0.1 ns is primarily due to holes drifting into the left contact ($V > 0$) or the right contact ($V < 0$).

Figure 4 shows the average current as a function of voltage bias. The error bars show the range of average current between the first half and the second half of the simulation. It is clear that with zero bias, the current is non-zero; this phenomenon has also been observed experimentally [12].

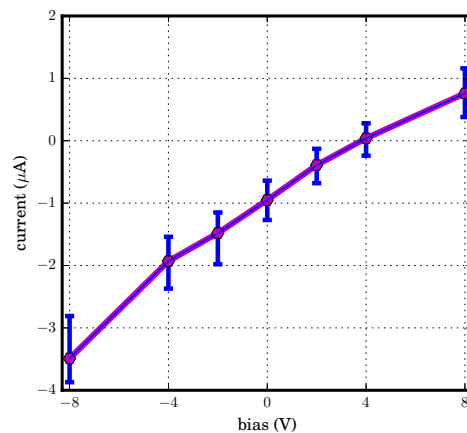


Figure 4: Average current as a function of voltage bias. The error bars show the range of current values over 1 ns.

SUMMARY

We first simulated a diamond detector where there is no potential barrier for charge carriers entering the metal contacts. In this case, the absorption of a photon generates a current which is linear in the applied voltage bias. In particular, we do not expect any current when there is no voltage bias. This is true even though in our simulations the electrons and holes do not drift at the same rate. When a potential barrier is added for electrons entering the metal contacts, the current is non-zero even when no voltage bias is applied.

REFERENCES

- [1] R. S. Sussmann, Ed., CVD Diamond for Electronic Devices and Sensors, John Wiley & Sons (2009).
- [2] http://henke.lbl.gov/optical_constants/atten2.html
- [3] D.A. Dimitrov et. al., J. Appl. Phys., **108**, 073712 (2010).
- [4] S. Tanuma, C. J. Powell and D.R. Penn, Surf. Interface Anal. **11**, 577 (1988).
- [5] C. Jacobini and L. Reggiani, Rev. Mod. Phys., **55**, 645 (1983).
- [6] J. Smedley et. al., in Diamond Electronics and Bioelectronics – Fund. to Appl. III, MRS Symposia Proceedings No. 1203, edited by P. Bergonzo et al., Mat. Res. Soc., Warrendale, PA, 1203-J17-21 and 1203-J19-03 (2010).
- [7] J. W. Keister et. al., IEEE Trans. Nucl. Sci. **57**, 2400 (2010).
- [8] G. P. Gilfoyle, Comput. Phys. Commun. **121**, 573 (1999).
- [9] A. F. J. Levy, Applied Quantum Mechanics, Cambridge University Press (2003).
- [10] M. Razavy, Quantum Theory of Tunneling, World Scientific, (2003).
- [11] D.A. Dimitrov et. al., J. Appl. Phys., **117**, 055708 (2015).
- [12] E. Muller, pers. comm. (2015).